Indian Journal of Fibre & Textile Research
Vol. 50, March 2025, pp. 41-47
DOI: 10.56042/ijftr.v50i1.7095

Efficient liquid transport fabric for active sports

Sofien Benltoufa[1,a]& Ayman Alfaleh[2]

[1]Laboratory for the Study of Thermal and Energy Systems (LESTE, LR99ES31), National Engineering School of Monastir, University of Monastir, Tunisia, 05000, Monastir, Tunisia

[2] College of Engineering and Computing, Mechanical and Industrial Engineering Department, Umm Al-Qura University, Al-Khalidiya District Al-Qunfudhah City 28821, Kingdom of Saudi Arabia

Received 4 December 2023; revised received and accepted 10 July 2024

This study designs an embossed jersey structure for fast liquid dissipation in highly active sportswear and workwear. Unlike conventional fabrics, where droplet diameter increases over time due to surface spreading, the newly designed fabric enables liquid absorption without lateral spreading, promoting efficient moisture evacuation. The structural parameters of polyamide 66 knitted fabrics are assessed for moisture transport in two forms: liquid and vapour. The comfort performance of the embossed structure is compared with simple jersey and interlock structures based on droplet kinetics and breathability. Droplet spreading behaviour is analysed through contact angle variation, droplet diameter, and droplet height as a function of time. Breathability is evaluated using water vapour permeability and air permeability measurements. The results show that the embossed jersey structure allows liquid dissipation without spreading, helping to prevent liquid diffusion and condensation. The jersey structure exhibits faster liquid wicking and higher water vapour and air permeability. Fabrics with higher porosity demonstrate superior breathability and moisture transport, contributing to improved physiological comfort.

Keywords: Air permeability, Breathability, Droplet kinetics, Embossed jersey, Water vapour permeability

1 Introduction

Understanding the transport of moisture in porous media is crucial for a variety of applications[1,2]. The textile industry, especially sportswear, is particularly interested in this process[3,4]. The comfort and performance of athletes depend on the textiles used for sportswear[1], especially the layer worn directly on the skin. To respond to internal and external influences, it is vital to regulate key physiological clothing parameters, including temperature, moisture, and air circulation)[5,6]. Moisture transport behaviour is a crucial factor in textile development[7]. During physical activity in hot and humid environments, clothing should allow rapid moisture removal[8]. Failure to do so can disrupt the body's heat balance and lead to skin damage and microbial growth[9]. Additionally, inadequate moisture removal can lead to fabric sticking to the skin, causing discomfort[10].

The heat and moisture transport properties of fabrics primarily determine thermophysiological comfort. Moisture may exist in both vapour and liquid forms, and its movement through textiles occurs via three principal mechanisms: diffusion of moisture due to the vapour gradient[11], sorption-desorption due to hydrophilic sites on the fabric, and forced convection driven by airflow near the skin[12].

Several studies have examined the absorption and spreading behaviour of liquids on porous materials[13-15], demonstrating that liquid transport is governed by surface tension, gravity, and viscous forces[16]. The wetting of materials is characterised by the contact angle[17]. A contact angle less than 90° indicates favourable wetting, while angles greater than 90° indicate unfavourable wetting. Wettability is typically assessed using the static contact angle[18], but some researchers have used the dynamic contact angle and capillary rise method to evaluate hydrophilicity[19]. However, these studies often neglect the effect of surface roughness on moisture transport[20].

In addition to contact angle-based methods, various techniques have been employed to assess moisture transport properties in textiles[21]. The Moisture Management Tester (MMT) is widely used to characterise the fluid transport properties of the fabric[22], while water vapour permeability measurements provide insights into a fabric's ability to facilitate evaporative cooling[23]. The latter is particularly relevant for

[a]Corresponding author.
E-mail: Sofien.benltoufa@enim.u-monastir.tn

maintaining thermal equilibrium[24], as efficient vapour transmission is essential to support body heat dissipation and ensure a comfortable microclimate between the skin and the fabric[25]. Fabric properties such as thickness, mass per unit area, and porosity significantly influence moisture transport and thermal comfort[26,27].

Given the importance of rapid moisture evacuation in sportswear, quick liquid-wicking fabrics play a pivotal role in enhancing wearer comfort and athletic performance. Despite the extensive literature on moisture transport mechanisms, a comprehensive method for characterising the full spectrum of physiological comfort parameters in quick liquid-wicking textiles remains lacking. Among high-performance fibres, polyamide 66 (PA 66) is widely used in sportswear due to its superior mechanical and moisture management properties[28].

This study aims to determine the comfort of PA 66 fabrics by assessing their moisture evacuation capacity in relation to fabric structure, total porosity, and mass per unit area. The liquid transport behaviour was characterised using contact angle measurements alongside droplet diameter kinetics, and spreading height analysis. However, liquid-phase moisture transport alone does not fully simulate the human body's interaction with the external environment. Therefore, in the second part of this study, breathability was examined through water vapour permeability and air permeability measurements to provide a more comprehensive understanding of fabric comfort.

2 Materials and Methods

2.1 Materials

Five types of knitted PA 66 fabrics were developed for sportswear applications. To vary the fabric's weight per unit area, fabrics A, B and C were knitted using 78/2 dTex nylon and 30D pure Spandex yarn, whereas fabrics D and E were knitted using 78/1 dTex nylon and 30D pure Spandex yarn. Both yarn compositions are regularly used in high-elastic garments, where Spandex serves as the ground yarn and nylon forms the veil.

The fabrics were knitted using five different structures frequently employed in seamless garments, utilising a Santoni seamless garment circular knitting machine (SM8-TOP2 MP2). Before testing, all samples were scoured using non-ionic synthetic detergents (1.5-2.0 g/L) along with an alkali (0.5–1.5 g/L sodium carbonate or trisodium phosphate) and subsequently relaxed using a RELAXLAB, according to the standard NF G 07 102. The knitted structures, material weights, thicknesses and total porosity are listed in Table 1.

2.2 Methods

The mass per unit area of the fabric was determined following the standard ISO 3801:1977.

The ISO: 5084 standard was used to measure the thickness of fabric samples. Total Porosity (ε) is characterised by the volumetric ratio of accessible pores to total volume. The porosity values were calculated using the following equation:

$$\varepsilon_{Total}(\%) = \left(1 - \frac{M}{\rho \times t_h}\right) \times 100 \qquad \ldots(1)$$

where M is fabric mass per unit area; t_h, thickness of the fabric; and ρ,fibre density.

2.1.1Droplet Dispersion Kinetic Measurement

The equilibrium contact angle of a liquid on an ideal solid surface follows Young's equation[29]:

$$\cos\theta = \frac{\gamma_{SV} - \gamma_{SL}}{\gamma_{LV}} \qquad \ldots(2)$$

where γ is interfacial tension of the solid-liquid (SL), solid-vapour (SV) and liquid-vapour (LV) interfaces.

The kinetic spreading parameters were analysed using water droplets, and the evolution of the droplet profile was recorded at 25 frames per second using a GBX Digidrop video camera. The Digidrop device uses a goniometric method to calculate the contact angle between a liquid and a solid. The droplet image was captured by a monochrome video camera, and the contact angle was computed using PC-based control acquisition and data processing. The water droplet was measured

Table 1 — Fabrics characteristics

Fabric code	Fabric structure	Knitting machine gauge (needle/inch)	Yarn count (dTex)	Mass per unit area (g/m^2)	Thickness (mm)	Wales per cm	Courses per cm	Total porosity (%)
A	Jersey	40	78x2	237±1.1	1.02±0.02	19± 1	18±1	79.61±2
B	Interlock	40	78x2	232±1.2	0.91±0.04	17± 1	18±1	77.63±2
C	Embossed Jersey	40	78x2	300±1.4	1.24±0.11	19± 2	18±1	78.77±3
D	Jersey	40	78x1	123±1.0	0.68±0.02	19± 1	20±1	84.14±1
E	Jersey	28	78x1	72±1.0	0.53±0.02	14± 1	13±1	88.08±3

directly with a video camera and calculated from the height and base diameter of the droplet. Distilled water was used as the working fluid in this work. The volume of water used was 5 μL, and each measurement was repeated five times.

2.1.2 Air Permeability Measurement

The air permeability of the fabrics in the transverse direction was measured using the FX3300 (Textest, Switzerland) instrument, according to ISO 9237 standard[30].

2.1.3 Water Vapour Permeability Measurement

The water vapour permeability was evaluated using the Permetest instrument as per ISO 11092, and the water vapour resistance (Ret) and thermal resistance (Rct) were also determined as per ISO 11092[31].

The device employed a heated porous membrane to simulate sweating skin. The heat flow required for water evaporation from the membrane was measured, with and without a fabric cover[32]: The measuring head was first covered with a semipermeable film to keep the measured material dry. The heating power value (U_0) was recorded without a sample. Then, the textile sample was inserted between the head (on the top of the semipermeable film) and the opening at the bottom of the channel. When the heating power signal stabilised, the value of (U_s) was recorded, which quantified the heat losses of the wet sensing head covered by the sample.

The instrument also measured the water vapour relative permeability (Pwv), calculated using the following equation:

$$P_{wv}[\%] = 100 \times \frac{U_s}{U_0} \quad \ldots(3)$$

All tests were carried out under standard atmospheric conditions of 20±2˚C and 65±4 % relative humidity, according to standard ISO 139:2005.

3 Results and Discussion

3.1 Droplet Kinetic Spreading

The droplet impact behaviour on the tested fabrics is analysed to assess their moisture management properties. Figure 1 depicts the droplet profile and changes in contact angle for different fabric samples.

All samples exhibit complete wettability, with equilibrium contact angles (θ_{eq}) reaching 0°, indicating full absorption. This characteristic is critical for sportswear materials, as efficient moisture absorption enhances wearer comfort. The absorption process begins when a droplet makes contact with the fabric surface, and its spreading behaviour is dictated by the static contact angle. Meanwhile, the dynamic contact angle provides a more realistic representation of moisture diffusion and absorption during wear.

Differences in droplet profiles are observed across the tested samples. The initial contact angle (θ_0),

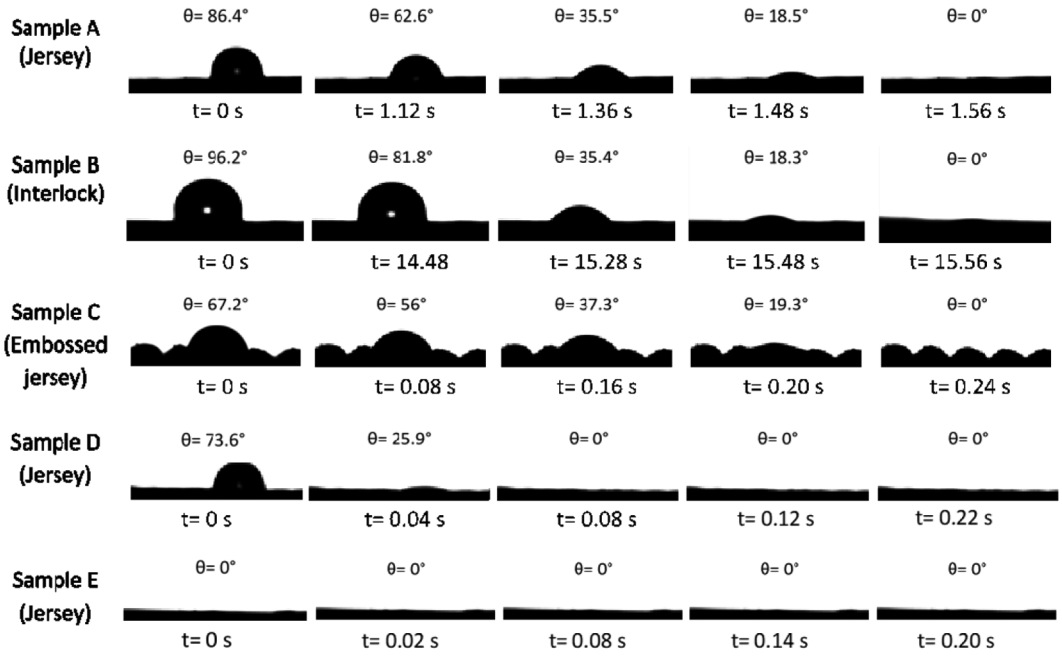

Fig. 1 — Droplet profile and contact angle variation of different fabrics

which describes the droplet's first interaction with the fabric surface, varies among the samples. Notably, sample B (interlock structure) is the only fabric where θ_0 exceeds 90°, suggesting a rough and void-filled surface. As the droplet interacts with the fabric, it gradually seeps into surface cavities, impacting its overall spreading and absorption behaviour[33]. The total spreading time, an important parameter for evaluating moisture comfort, differs across samples. However, this metric alone does not fully characterise the fabric's moisture transport efficiency. To provide deeper insight, contact angle kinetics are analysed alongside droplet dispersion (t). The dimensionless diameter ($D(t)/D_0$) and dimensionless height ($h(t)/h_0$) of the droplet over time are also examined to establish a correlation between fabric structure and moisture transport efficiency.

3.1.1 Effect of Fabric Structure

As seen in Fig. 1, sample B exhibits a two-phase change in contact angle over time. The first phase (0 s to 14.48 s) shows a nearly constant contact angle, followed by a second phase (14.48 s to 15.58 s) where the contact angle decreases until reaching equilibrium at 0°. The initial phase allows the liquid to penetrate macropores (cavities between yarns), which act as reservoirs for mesopores (spaces between fibres) once saturated[14]. While a spreading time of 14.48 s may be sufficient for low-intensity activities, it is inadequate for high-performance conditions where a higher sweating rate can lead to fabric saturation and discomfort.

Fabric structure plays a critical role in moisture dispersion. In interlock structures, the first phase dominates, requiring 15.58 s to reach an equilibrium contact angle of 0°. In contrast, the jersey and embossed jersey fabrics transition to the second phase more quickly, allowing faster liquid spread. This behaviour is attributed to the lower porosity of interlock structures compared to jersey fabrics of similar weight (Table 1). The tightly packed structure of interlock fabrics increases liquid-solid interactions, reducing the liquid-air interface and slowing moisture absorption.

In jersey fabrics, larger and more connected pores allow for improved moisture absorption. The surface forces acting on the droplet influence the resistance in the first phase of absorption. The second phase, characterised by rapid absorption, is accelerated by pre-wetting film formation and the reduction of surface tension. Among jersey variants, embossed jersey fabrics exhibit the fastest liquid diffusion. The equilibrium contact angle is achieved at 0.24 ± 0.03 s for embossed jersey, compared to 1.56 ± 0.05 s for standard jersey. This is attributed to microcavities in the embossed structure (Fig. 2), which increase the liquid-air interface and enhance moisture diffusivity.

Since the contact angle only describes surface absorption, additional analysis is conducted to examine droplet penetration into the fabric thickness. The adimensional diameter and height variations provide further insights into moisture transport within macro- and mesopores.

As seen in Fig. 3, the two-phase spreading model is confirmed. In interlock fabrics (B), D/D_0 remains constant before gradually decreasing to equilibrium at 0°, whereas in jersey (A) and embossed jersey (C) fabrics, liquid penetration occurs more rapidly. In embossed jersey (C), both D/D_0 and droplet height decrease over time, indicating that moisture diffuses into the fabric rather than spreading along its surface. This supports the notion that macropore diffusion dominates over thickness-wise moisture evacuation[14]. The cavities in embossed jerseyfabrics act as reservoirs, facilitating rapid liquid absorption and transport through the fabric.

The configurations illustrated in Fig. 4 define the difference between droplet spreading on the fibre surface (Case 1) and direct penetration into macropores (Case 2).

Droplet penetration without spreading (Case 2) is preferable under conditions of high perspiration, as it

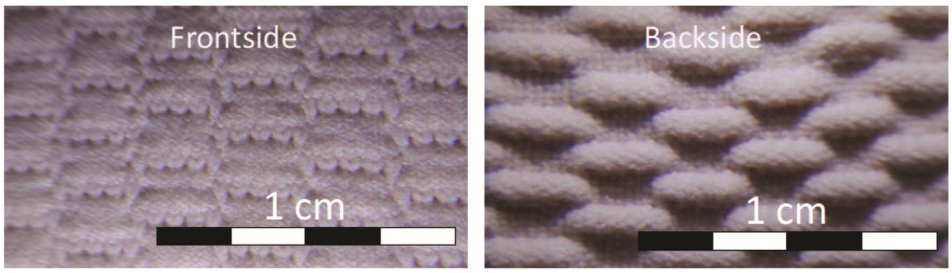

Fig. 2 — Microscopic view of front and back side of embossed jersey knitted fabric

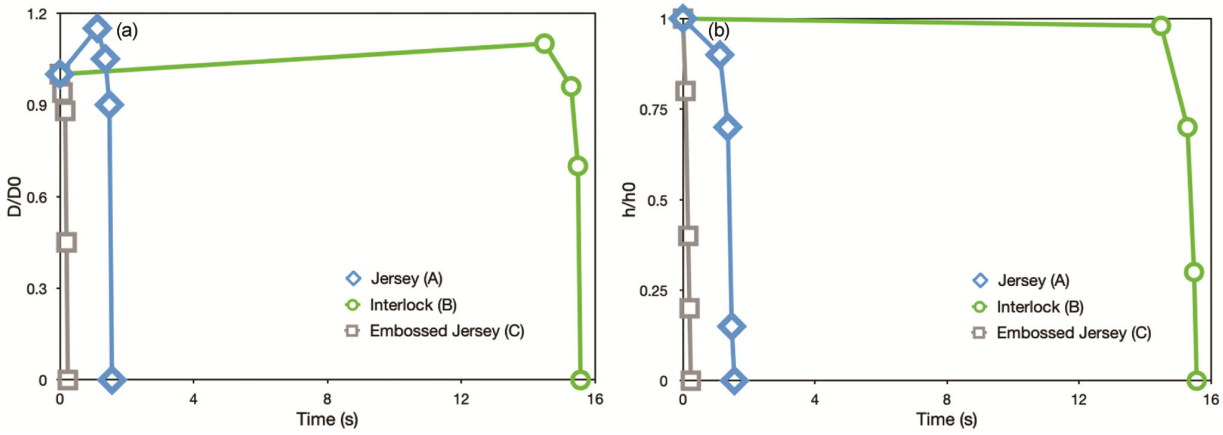

Fig. 3 — Comparison of different knitted structures (a) adimensional diameter and (b) adimensional height

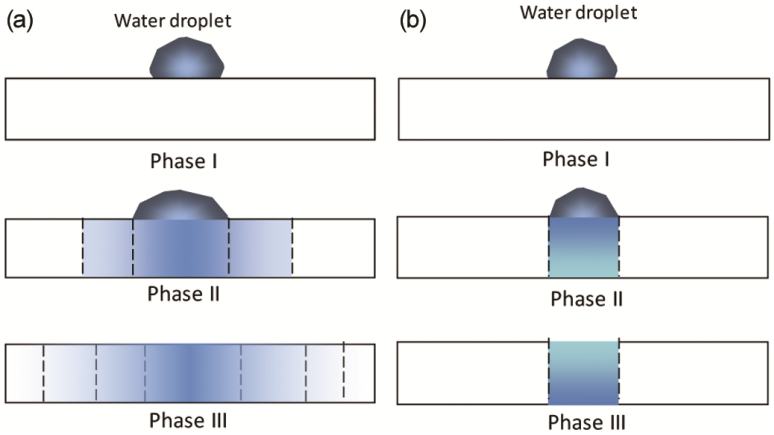

Fig. 4 — Droplet spreading configurations over fibrous media: (a) case 1 (drop spreading) and (b) case 2 (drop penetration without spreading)

enables rapid liquid evacuation to the fabric's outer layer. This mechanism prevents a liquid saturation on the fabric surface, which could otherwise block the liquid passage to the outer layer.

3.1.2 Effect of Fabric Mass Per Unit Area

The impact of fabric mass per unit area on moisture transport is examined using three jersey samples with different weights (237±1.1 g/m^2, 123±1.0 g/m^2, 72 ± 1.0 g/m^2) (Fig. 1). Samples A, D, and E have the same fabric composition and structure, but their weights vary to assess the impact on liquid diffusion kinetics (in this case, the droplet). The results indicate that sample E (72 g/m²) facilitates immediate liquid diffusion, reaching θ_{eq} = 0° at 0 s, with a standard deviation of 0.2° and a CV of 3.2%. This behaviour is attributed to its high total porosity (88.08±3.8%), which enhances moisture transfer.Conversely, sample A (237 g/m²) exhibits slower diffusion due to its denser structure (total porosity = 79.61±2 %). The higher stitch density (19 ± 1 wales/cm × 18 ± 1 courses/cm) in sample A increases fabric compactness, restricting droplet diffusion. In contrast, samples D (stitch density=19±1 wales/cm x 20±1 courses/cm) and E (stitch density=14±1 wales/cm × 13±1courses/cm), with larger mesopores, facilitate faster spreading kinetics.

Pore size differences further explain the observed trends. In samples D and E, larger surface pores allow immediate droplet penetration, whereas, in sample A, smaller pores result in initial surface spreading before absorption. The kinetic diffusion patterns in Fig. 5 illustrate that droplet penetration is slower in denser fabrics, as the liquid must first spread across the surface before diffusing into the structure.

The droplet diameter and height decrease as the fabric's mass per unit area increases. In sample A, the droplet diameter initially increases, then remains constant, and finally reduces as it penetrates the fabric. At the first-time laps, the diameter increases

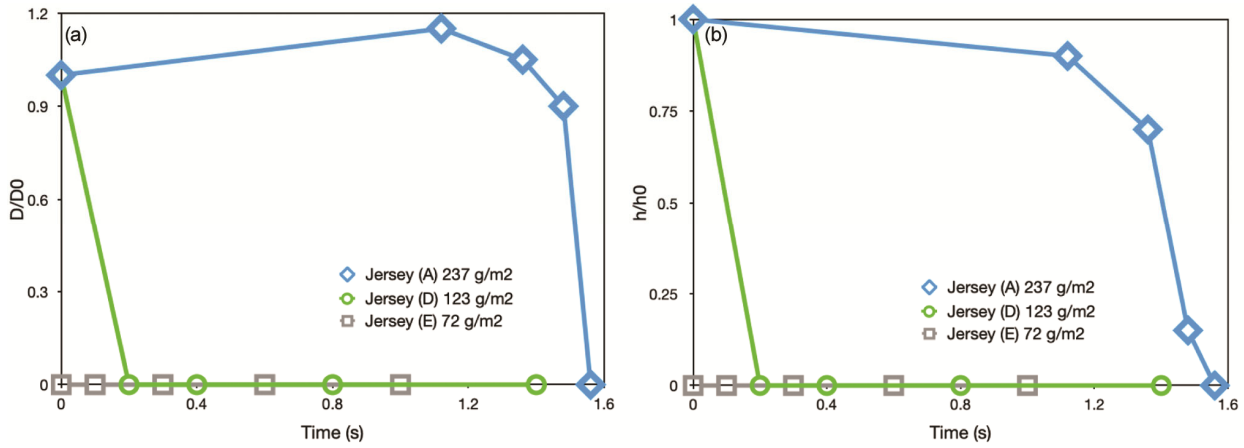

Fig. 5 — Variations in diameter and height of simple jersey structure for different fabric mass per unit area

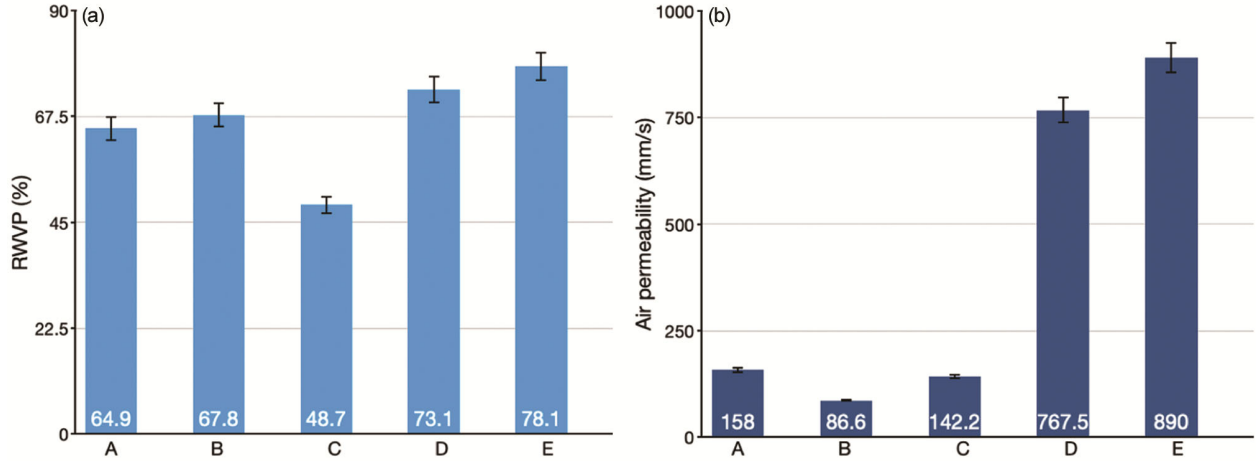

Fig. 6 — Breathability: (a) Relative water vapour permeability (%), and (b) air permeability (mm/s)

due to droplet spreading and penetration. In samples D and E, however, the diameter decreases immediately upon contact, as larger pores prevent diffusion without spreading. In the heavier fabric (sample A), narrower pores facilitate droplet penetration, leading to spreading and absorption by macro pores, which serve as reservoirs for mesopores during the second wetting phase[14].

The findings confirm that fabric weight influences moisture transport. Heavier fabrics exhibit slower spreading rates due to reduced porosity and increased liquid-solid interaction, leading to prolonged moisture retention. This can negatively impact wearer comfort, making lighter, more porous fabrics preferable for high-performance applications.

3.2 Fabric Breathability

Breathability is assessed using relative water vapour permeability (RWVP) and air permeability measurements, as presented in Fig. 6.

Sample E exhibits the highest water vapour permeability (78.1%), with a CV of 2.9%, while sample C (embossed jersey) demonstrates the lowest (48.7%). This difference is attributed to the structure of the embossed jersey, which, despite facilitating liquid transport, traps water vapour within its cavities, reducing vapour permeability.

A comparison of samples A and C further supports this observation. The standard jersey structure exhibits higher water vapour permeability (64.9%) than the embossed jersey (48.7%), indicating that open pores facilitate vapour transport more effectively than profiled cavities. Sample E, the lightest fabric, also exhibits the highest air permeability (890 mm/s), with a CV of 5.1%, reinforcing the correlation between fabric porosity and breathability.

4 Conclusion

This study aims to assess the comfort parameters of a newly developed fabric that quickly evacuates

liquid. It investigates the influence of fabric structure and mass per unit area on moisture transport and breathability in knitted PA 66 fabrics designed for sportswear applications. The results demonstrate that fabric structure significantly affects droplet spreading kinetics, absorption behaviour, and overall moisture management.The embossed jersey structure exhibits the fastest moisture diffusion due to its well-defined cavities, which enhance liquid absorption and rapid transfer through the fabric thickness. In contrast, the interlock structure shows slower spreading kinetics, with liquid retention occurring in the surface macropores before diffusing into the mesopores. This delay in moisture evacuation suggests that interlock fabrics may be less suitable for high-performance sportswear where rapid sweat removal is essential.The study further confirms that fabric mass per unit area is crucial in moisture transport. Lighter fabrics with higher porosity facilitate immediate droplet absorption and enhanced water vapour permeability. Breathability analysis reinforces these findings, highlighting the importance of total porosity in regulating thermal comfort. While embossed jersey structures excel in liquid-phase moisture transport, their vapour permeability remains lower than standard jersey fabrics due to water vapour entrapment within structured cavities. This suggests that a balance between macropore-driven liquid transport and vapour diffusion is necessary for optimal comfort. The results emphasise that fabric selection for sportswear should prioritise structures that enable rapid liquid transport while maintaining high vapour permeability. Investigating moisture spread through the outer layer of textiles and the influence of material parameters on evacuation remains an important area for future research.

References

1 Manshahia M & Das A, *Fibre Polym*, 15 (2014) 6, doi:10.1007/s12221-014-1221-9.

2 Das A, Kothari V K & Sadachar A, *Fibre Polym,* 8 (2007) 1, doi:10.1007/BF02908169.

3 Senthilkumar M, Sampath M B , Ramachandran T, *J Inst Engg (India): E,* 93 (2012) 2, doi:10.1007/s40034-013-0013-x.

4 Wei Y, Li J & Li Y, *Polym Test,* 59 (2017), doi:10.1016/j.polymertesting.2017.01.019.

5 Troynikov O & Wardiningsih W, *Text Res J,* 81 (2011) 6, doi:10.1177/0040517510392461.

6 Chen Q, Miao X, Mao H, Ma P & Jiang G, *ARJ,* 16 (2016) 6, 10.1515/aut-2015-0034.

7 Zhang C, Wang X, Lv Y, Ma J & Huang J, *Polym Test*, 29 (2010) 5, doi:10.1016/j.polymertesting.2010.02.004.

8 Dong Y, Kong J, Mu C, Zhao C, Thomas N L & Lu X, *Mater Des*, 88 (2015), doi:10.1016/j.matdes.2015.08.107.

9 Çil M G, Nergis U B & Candan C, *Text Res J,* 79 (2009) 10, doi:10.1177/0040517508099919.

10 Huang J, *Polym Test*, 25 (2006) 5. doi:10.1016/j.polymertesting.2006.03.002.

11 Charaka A, Berger J, Benmahiddine F & Belarbi R, *Int J Heat Mass Transf*, 209 (2023), doi:10.1016/ j.ijheatmasstransfer.2023.124122.

12 Bal K & Das B, *Functional and Technical Textiles*, Elsevier; 2023:453-498, doi:10.1016/B978-0-323-91593-9.00014-6.

13 Kissa E, *Text Res J,* 66 (1996) 10, doi:10.1177/ 004051759606601008.

14 Benltoufa S, Fayala F & BenNasrallah S, *J Eng Fiber Fabr*, 3 (2008) 3,doi:10.1177/155892500800300305.

15 El Messiry M & Fadel N, *Text Res J,* 90 (2020) 2, doi:10.1177/0040517519866947.

16 Huang E, Skoufis A & Denning T, *J Open Source Softw*, 6 (2021) 58, doi:10.21105/joss.02604.

17 Sygusch J & Rudolph M, *Appl Surf Sci*, 566 (2021), doi:10.1016/j.apsusc.2021.150725.

18 Kumar S M & Deshpande A P, *Colloids Surf A Physicochem Eng Asp*, 277 (2006) 1, doi:10.1016/j.colsurfa.2005.11.056.

19 Wei Q, Liu Y, Hou D & Huang F, *J Mater Process Technol*, 194 (2007) 1, doi:10.1016/j.jmatprotec.2007.04.001.

20 Julien E, Rubinstein S M, Caré S & Coussot P, *Soft Matter,* 19 (2023) 19, doi:10.1039/d3sm00229b.

21 Das B, Das A, Kothari V K, Fangueiro R & de Araújo M, *ARJ,* 7 (2007) 3.

22 Yao B, Li Y, Hu J, Kwok Y & Yeung K, *Polym Test,* 25 (2006) 5, doi:10.1016/j.polymertesting.2006.03.014.

23 Bedek G, Salaün F, Martinkovska Z, Devaux E & Dupont D, *Appl Ergon*, 42 (2011) 6, doi:10.1016/j.apergo.2011.01.001.

24 Chan A P C, Guo Y P, Wong F K W, Li Y, Sun S & Han X, *Ergonomics,* 59 (2016) 4, doi:10.1080/00140139.2015.1098733.

25 Huang J, *Text Res J,* 86 (2016) 3, doi:10.1177/004051 7515588269.

26 Ramratan R & Choudhary A K, *JTATM,* 11 (2020) 2.

27 Benltoufa S, Fayala F, Cheikhrouhou M & Nasrallah B, *ARJ,* 7 (2007) 1.

28 Coutinho C, Duarte A & Sanches R, *Comparative Study of the Comfort Promoted by the Use of Garments Made of Polyamide and Polyester Fibers during the Practice of Running*, CRC Press; 2020, doi:10.1201/9780429286872-66.

29 Govindharajan S, Raman S, Shanmugam V, Rathanasamy R & Palaniappan S K, *Materialpruefung/Materials Testing*, 63 (2021) 11, doi:10.1515/mt-2021-0038.

30 391 T, 9237 EI. Determination of Permeability of fabrics to air. *Textiles*, Published online 1999:1-8.

31 ISO 11092. Measurements of thermal and water-vapour resistance under steady-state condition, 2014, 1.

32 Hes L & Carvalho M, *Indian J Fibre Text Res,* 19 (1994) 3.

33 Espín L & Kumar S, *J Fluid Mech,* 784 (2015), doi:10.1017/jfm.2015.603.